Removal of sulphate from mine waters by electrocoagulation/rice straw activated carbon adsorption coupling in a batch system: optimization of process via response surface methodology

Mijia Zhu, Xianqing Yin, Wu Chen, Zhengji Yi and Heyong Tian

ABSTRACT

The removal of sulphate ions constitutes one of the main challenges in mining, metallurgical and other industries. This work evaluated sulphate removal from aqueous solutions by an electrocoagulation (EC)/raw straw activated carbon (RSAC) adsorption coupled process. The process parameters affecting sulphate removal efficiency were investigated: current density (0–100 mA/cm^2), RSAC dosage (0–0.8 g/L), initial pH (4–9) and reaction time (0–40 min). A central composite design coupled with response surface methodology (RSM) was used to construct a mathematic model of EC/RSAC process that considers three key variables, namely current density, RSAC dosage and reaction time. Under optimum conditions (current density of 75 mA/cm^2, dosage of 0.46 g/L and reaction time of 19.2 min), the removal efficiency of sulphate reached 95.2%. The RSM predictive value was 94.08% with a small deviation (1.12%). Thus, the fundamental data and results can provide some useful information for further studies and applications of the EC/RSAC coupled system in sulphate-containing wastewater treatment.

Key words | electrocoagulation, mine wastewater, raw straw activated carbon, response surface methodology, sulphate ions

Mijia Zhu (corresponding author)
Xianqing Yin
Wu Chen
School of Chemistry and Environmental Engineering,
Yangtze University,
Jingzhou 434000,
China
E-mail: *zhumijia128@163.com*

Zhengji Yi
Key Laboratory of Functional Metal-Organic Compounds of Hunan Province and Key Laboratory of Functional Organometallic Materials of College of Hunan Province, Department of Chemistry and Material Science,
Hengyang Normal University,
Hengyang 421008,
China

Heyong Tian
HQC (Xinjiang) Company,
Urumqi 830000,
China

INTRODUCTION

Mine water is a source of sulphate contamination of natural water and industrial wastewater (Najib *et al.* 2017). The presence of sulphate (SO_4^{2-}) in mine water is associated with the oxidation of sulphides and elemental sulphur or chemical weathering of sulphur-containing minerals when the drainage is exposed to oxygen and water (Kefeni *et al.* 2017). As a result, this drainage is often characterised by a low pH and high sulphate concentration (Papirio *et al.* 2013). High sulphate ion concentration (>600 mg/L) can affect the taste of drinking water and lead to diarrhea (Silva *et al.* 2012; Najib *et al.* 2017). Moreover, this type of water can cause erosion of metal parts in water delivery systems, and boilers and heat exchangers (Silva *et al.* 2010; Najib *et al.* 2017). Several technologies are available for the removal of SO_4^{2-}, including chemical precipitation (Iii & Trahan 1999), biological degradation (Greben *et al.* 2009; Martins *et al.* 2009), ion exchange (Guimarães & Leão 2014), electrochemical method (Gärtner *et al.* 2005; Paz-García *et al.* 2013) and adsorption methods (Namasivayam & Sangeetha 2008). Some of these methods are limited because sulphate removal is a complex problem due to the high solubility and stability of SO_4^{2-} in aqueous solutions (Namasivayam & Sangeetha 2008; Silva *et al.* 2010; Runtti *et al.* 2017). Electrocoagulation (EC) can be used to remove

doi: 10.2166/wrd.2018.054

sulphate ions from mining waters (Mamelkina *et al.* 2017). This method has advantages over others for contaminated water remediation because it requires relatively simple equipment, is easy to automate, needs no additional reagents and has high efficiency with a short operation time (Kumar *et al.* 2004; Guvenc *et al.* 2017).

In EC, the coagulants are generated *in situ* by the electrooxidation of metal electrodes. Owing to the high coagulation efficiency of Al^{3+} ions, aluminium is applied as the sacrificial anode (Zhu *et al.* 2016b). These metal ions can form aluminium hydroxide species, which neutralise negatively charged contaminants, such as SO_4^{2-}. The formed flocs are then separated from the contaminated water by sedimentation or flotation (Elnenay *et al.* 2017; Franco *et al.* 2017). Chemical reactions at the anode are shown in Equations (1)–(4):

$$Al_{(s)} \rightarrow Al^{3+}_{(aq)} + 3e^- \quad (1)$$

$$2H_2O_{(l)} \rightarrow O_{2(g)} + 4H^+_{(aq)} + 4e^- \quad (2)$$

$$Al^{3+}_{(aq)} + 3H_2O_{(l)} \rightarrow Al(OH)_{3(aq)} + 3H^+_{(aq)} \quad (3)$$

$$nAl(OH)_{3(aq)} \rightarrow Al_n(OH)_{3n(aq)} \quad (4)$$

The reaction at the cathode is described as:

$$2H_2O_{(l)} + 2e^- \rightarrow H_{2(g)} + 2OH^-_{(aq)} \quad (5)$$

EC is an emerging water treatment technology that has already been used to treat various wastewaters from restaurants (Chen *et al.* 2007), the textile (Bayramoglu *et al.* 2004), paper (Zaied & Bellakhal 2009), and metal plating industries (Akbal & Camc 2011), as well as from slaughterhouses (Kobya *et al.* 2006). However, the easy formation of an impermeable oxide film on the cathode using the conventional EC process results in high operation cost and low efficiency (Avsar *et al.* 2007). Recently, numerous methods have been undertaken to enhance conventional EC systems. For example, Vivek & Ganesan (2009) reported that an EC system coupled with granular activated carbon adsorption was more efficient and yielded faster separation compared with the conventional EC alone. Given that adsorption products are abundant in nature, agricultural wastes or by-products are assumed to be relatively inexpensive adsorbents to reduce the preparation costs. Rice straw is present in large amounts in China. Farahmand *et al.* (2015) reported that rice straw activated carbon (RSAC) can be used as an adsorbent to remove sulphate from effluents. It is not known whether EC can be coupled with RSAC adsorption as a feasible new technology to remove sulphate from mine wastewaters.

Therefore, we investigated the removal of sulphate from an aqueous solution using the EC/RSAC coupled method. The sulphate removal efficiency was selected as the response variable, and the effect of current density, dosage of RSAC, pH and reaction time on the removal efficiency were characterized. The parameters were optimized using a response surface methodology (RSM), which evaluates the interactions of multiple parameters on the response variable. Functional relationships between the response variable and the parameters were estimated. The results reported here will be helpful to the design of new EC/RSAC adsorption coupling systems for the future treatment of mine waters.

MATERIALS AND METHODS

Materials

Mine water was collected from the storage dam of a mining area in Magu (located in Guizhou Province, southwest China, sampling date 5/12/16) and stored in a freezer at −20 °C. The pH value was measured using an HQ11D pH meter (Hach Co., Ltd, Shenzhen, China). Total dissolved solids and electrical conductivity were monitored using a Eutech Instruments CON510 conductivity meter (Vensik Electronics Co., Ltd, Qidong, China) at the temperature of 25 ± 0.2 °C. Cation analysis was performed using an inductively-coupled plasma-atomic emission spectrometry (ICP-AES, HK8100, Huakeyitong Co., Ltd, Beijing, China) and inductively-coupled plasma-mass spectrometry (ICP-MS, Agilent 7900, Beijing, China). The former was used for concentrations greater than 1 mg/L, and the latter was used for concentrations less than 1 mg/L. Anion analysis was performed using ion chromatography (IC, ICS1000, Dionex Co., Ltd, Sunnyvale, USA). All samples were filtered

(Whatman No. 1) before the ionic analysis to avoid any interference by the deposit. The data are presented in Table S1 (available with the online version of this paper).

Rice straw was collected from the agricultural lands in Jingzhou City in the south of China. The agricultural wastes were minced in an electric mill and then washed three or five times with deionised distilled water. The RSAC was prepared using zinc chloride (purity ≥98%), as described by Farahmand *et al.* (2015). The obtained adsorbent was then sieved to 0.25–0.5 mm. The specific surface areas (338 m^2/g) were calculated from the N_2 isotherm data by Brunauer–Emmett–Teller equation. The pH_{pzc} (point of zero charge) is a key characteristic that determines the surface changes of the activated carbon. The pH_{pzc} (6.7) of RSAC was measured as previously described (Zhu *et al.* 2016a). The characterisations of RSAC were carried out by Fourier transform infrared spectroscopy (FTIR) and scanning electron micrograph (SEM). The spectrum of the samples was recorded in the range of 4,000–400 cm^{-1} using a Perkin Elmer Model spectrum 400 FTIR spectrometer in KBr pellets. The samples were dried at room temperature and coated with Au under vacuum in an argon atmosphere for the SEM analysis (SU8010, Hitachi, Tokyo, Japan).

Experimental setup

As shown in Figure 1, the EC/RSAC adsorption process was conducted in a 720 mL EC cell (12 × 10 × 6 cm) using an organic glass reactor. Aluminum (purity ≥99%) was used as sacrificial electrodes, and stainless steel was used for the cathode. The effective area of the each electrode plate was 20 cm^2. Parallel anodes and cathodes were positioned vertically, and separated at a certain distance. The electrodes were connected to a digital direct current (DC) power supply (WKY-505, East Co., Ltd, Guangdong, China) with voltage and electrical current range of 0–50 V and 0–5 A, respectively. Before each run, the electrodes were rubbed with fine-grained emery paper, washed with 0.2 M HCl and then with distilled water. For every experimental run, 600 mL of mine waters were placed into the EC reactor. The solutions were stirred constantly (200 rpm) using a magnetic stirrer. The current density, electrode gap, initial pH and reaction time were set to a desired value. The pH was adjusted by adding 0.1 M HCl or 0.1 M NaOH and measured using a HQ11D pH meter (Hach Co., Ltd, USA). All the runs were performed at room temperature (20 °C). The sulfate removal efficiency is defined as follows:

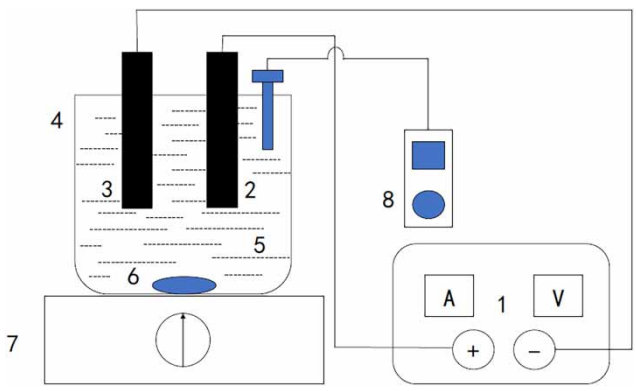

Figure 1 | Electrocoagulation equipment (1. Power source; 2. parallel anode; 3. parallel cathode; 4. electrocoagulation cell; 5. electrolysis solution; 6. magnetic bar stirrer; 7. magnetic stirrer; 8. pH meter).

$$\text{Removal efficiency, } \% = (C_0 - C_t)/C_0 \times 100\% \quad (6)$$

where C_0 and C_t are sulfate concentrations (mg/L) at time 0 and time t (min), respectively.

Experimental design and model development

The statistical software Design Expert 8.0 (Stat-Ease Inc., Minneapolis, USA) was applied for the experimental design, analysis and optimization. Central composite design (CCD) was employed to investigate and optimize the experimental variables in the sulfate removal from mine waters. Three independent factors, the current density (X_1), dosage of RSAC (X_2) and reaction time (X_3), were studied at five levels with five repetitions at the central point using circumscribed CCD.

CCD consists of 2^3 factorial designs augmented by six axial points coded as $\pm\alpha$ and three central points (all variables at zero level). The value of α was calculated as follows:

$$\alpha = 2^{n/4} \quad (7)$$

where n is the number of variables in CCD. Therefore, α is equal to $2^{3/4} = 1.682$ according to Equation (7). Each parameter was coded at three levels, −1.681 (minimum), 0 (central), and +1.681 (maximum), which covered the

entire study range. The range and levels of the three variables were measured with the equation:

$$X_i = (x_i - x_{ic})/\Delta x_i \quad (8)$$

where X_i stands for the dimensionless value of the ith test variable, x_i denotes the real value of the ith test variable, x_{ic} is the real value of the ith independent variable at the center point and Δx_i is the step size. Table 1 shows the CCD matrix.

The experimental data were analysed using the response surface regression equation to fit the following quadratic model:

$$Y = \beta_0 + \sum_{i=1}^{k} \beta_i x_i + \sum_{i=1}^{k} \beta_{ii} x_i^2 + \sum_{i=1}^{k} \sum_{j=1}^{k} \beta_{ij} x_i x_j + \varepsilon \quad (9)$$

where Y is the response; β_0 is a constant coefficient; ε is the error; and β_i, β_{ii} and β_{ij} are interaction coefficients of linear, quadratic and second-order terms, respectively. x_i and x_j are the coded independent variables. Subscripts i and j are the integer variables. The quality of the fit and the significance of the model were checked with the coefficient of determination (R^2) and Fisher's F-test, which were performed by analysis of variance (ANOVA) with 95% confidence level. After fitting the model, the generated data were used for 3D response surface optimization.

RESULTS AND DISCUSSION

Characterization of RSAC

Figure S1 (available with the online version of this paper) shows the FTIR spectrum of raw rice straw and activated carbon prepared from rice straw. The broad adsorption band at around 3,419.12 cm^{-1} can be attributed to the stretching of H-bonded hydroxyl groups. The adsorption peak at 2,926.20 cm^{-1} is assigned to C-H stretching vibration. The peak at 1,632.86 cm^{-1} is due to the bending vibration mode of the adsorbed water molecules. In contrast to raw rice straw, a sharp adsorption peak of the stretching vibration of C-N bond is observed at 605.57 cm^{-1} in RSAC (Farahmand *et al.* 2015). Representative SEM images of the raw and activated rice straw are shown in Figure S2 (available online). The surface morphologies of the activated material are clearly irregular and porous, which could favour a high uptake of sulphate.

Table 1 | Experimental ranges and levels of the independent variables

	Range and level				
Name of variables	−1.681 (low)	−1	0	+1	+1.681 (high)
Current density (mA/cm^2)	53.2	60	70	80	86.8
Dosage (g/L)	0.06	0.2	0.4	0.6	0.74
Reaction time (min)	6.6	10	15	20	23.4

Effect of current density

The current density is a crucial parameter that affects not only coagulant dosage but also influences the bubble formation rate, their size and flocs growth (Canizares *et al.* 2006). Various selected current densities: 0, 10, 20, 30, 40, 50, 60, 70, 80, 90 and 100 mA/cm^2, were applied during the batch experiment to establish a favourable range of current density for the EC/RSAC coupling process. A continuous EC process using an electrode pair of aluminium stainless-steel anode/cathodes was carried out at a reaction time of 30 min, and RSAC concentration of 0.2 g/L in the reactor was used to investigate the effect of current density on the sulphate removal efficiency. Compared with the RSAC adsorption process, EC/RSAC can significantly enhance the removal efficiency even at a low current density (10 mA/cm^2). As shown in Figure 2, the removal efficiency of RSAC adsorption process and EC/RSAC adsorption coupling process were 2.7 and 6.3% at 5 min and 17.5 and 54.2% at 30 min, respectively. The removal efficiency was improved likely due to the fact that the reaction in the coupled system is more complex than a simple RSAC adsorption process. The EC coupled with RSAC adsorption has a substantial effect on the sulphate removal efficiency (Carvalho *et al.* 2015). The results showed that the removal efficiency significantly increased with increasing current density. The highest removal efficiency (88.9%) was obtained at a current density of 70 mA/cm^2. This phenomenon could be ascribed to the fact that the amount of oxidised metal increased at high current densities, thereby resulting in a substantial amount of $Al(OH)_{3(s)}$ particles that favours the removal of pollutants (Sahu *et al.* 2014).

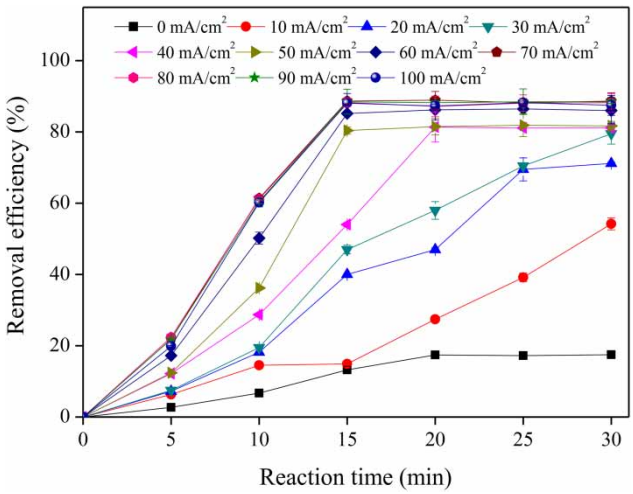

Figure 2 | Effect of current density on sulphate removal efficiency (conditions: reaction time 30 min; initial pH 6.5; RSAC dosage 0.2 g/L).

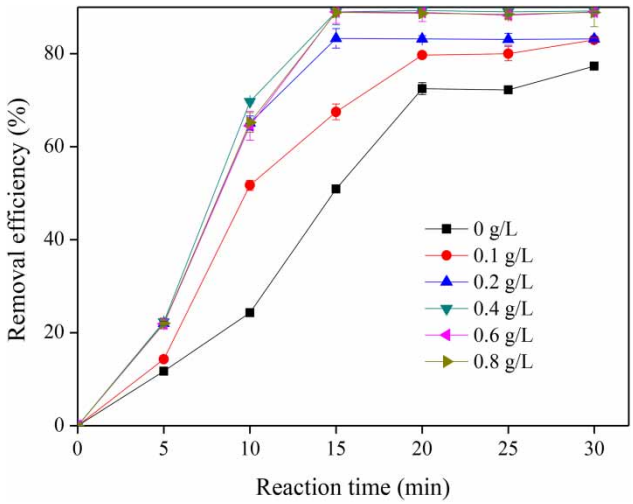

Figure 3 | Effect of RSAC dosage on sulphate removal efficiency (conditions: reaction time 30 min; current density 70 mA/cm^2; initial pH 6.5).

Figure 2 also shows a slight decline (from 88.7 to 87.3%) in the removal efficiency when the current density was up to 70 mA/cm^2. A similar phenomenon was observed in the study of Bayar *et al.* (2011), and such a similar trend may be explained by the increasing number of hydrogen bubbles at high current densities, which causes the coagulants to rapidly float on the aqueous phase surface and reduces the possibility of interaction between coagulants and pollutants. Based on the above studies, the ideal current density of 70 mA/cm^2 was used for subsequent experiments.

Effect of RSAC dosage

The effect of RSAC dosage was studied by changing the quantity of adsorbent range of 0–0.8 g/L. The other operational parameters were maintained constant (reaction time of 30 min and current density of 70 mA/cm^2). The results are presented in Figure 3, which shows that the removal efficiency was only 24.3% at the reaction time of 10 min without the presence of RSAC adsorption while the removal efficiency was 51.7% at 10 min with 0.1 g/L of RSAC. The available adsorption sites and the surface area increased by increasing RSAC dosage, thereby showing a dramatic increase in the sulphate removal efficiency at 15 min from 50.9 to 89.0% for an increase in RSAC dosage from 0.1 to 0.4 g/L. The extent of adsorption reaches a plateau when the dosage is greater than 0.4 g/L. This trend was anticipated because the adsorbed sulphate ions quantity per unit weight of the RSAC decreased by increasing the RSAC quantity. A similar phenomenon was also found in the study by Hallajiqomi & Eisazadeh (2017). Therefore, the optimum dosage was 0.4 g/L and was used for the rest of the single factor experiment.

Effect of initial pH

The effect of pH on the adsorption process is significant because pH affects the solubility of metal hydroxide and surface characteristic of the adsorbent material (Sundaramurthy *et al.* 2012; Zhu *et al.* 2016a). Batch experiments were conducted for the EC/RSAC coupled adsorption process at pH 4, 5, 6.5, 7, 8 and 9. The results presented in Figure 4 show that the maximum percentage sulphate removal (90.5%) was at neutral conditions, that is, pH 7. The sulphate removal efficiency was also low either at low or high pH. This is because at low pH (<4), the primary form of aluminum's occurrence is Al^{3+}, at high pH (>8), the primary form of aluminium hydroxide is $Al(OH)_4^-$. These products are not useful for adsorption. (Figure S3, available online, shows that the Al(III) species distribution could be estimating under a wide variety of pH values using MINTEQ 3.0.) A decline in sulphate removal efficiency (from 90.5 to 89.0%) was observed with an increase in pH (from 7 to 9). The pH can also affect the surface charge of RSAC. The suppressed removal efficiency is partly due to the electrostatic repulsion between the negatively charged surface of RSAC (pH > pH_{pzc}) and sulphate ions. According to

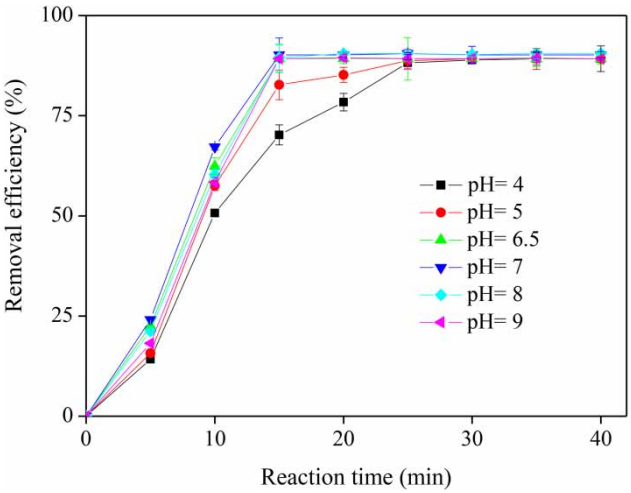

Figure 4 | Effect of initial pH on the sulphate removal efficiency (conditions: current density 70 mA/cm^2; RSAC dosage 0.4 g/L; reaction time 40 min).

the preceding analysis, the optimum pH for EC/RSAC coupled adsorption process was 7.

Regression model equation and analysis of variance

Table 2 shows the experimental results for the sulphate removal efficiency based on the CCD. The results of the ANOVA of the regression parameters of the predicted response surface quadratic model for sulfate removal efficiency are shown in Table S2 (available online). The relationship between sulfate removal efficiency and the three independent variables (i.e. current density, dosage and reaction time) was fitted to the second-order polynomial equation as given below:

$$Y = 90.42 + 4.6\,X_1 + 2.89\,X_2 + 9.9\,X_3 + 2.15\,X_1X_2 + 0.68\,X_1X_3 + 1.98\,X_2X_3 - 7.18\,X_1^2 - 4.17\,X_2^2 - 9.67\,X_3^2 \quad (10)$$

For the sulphate removal efficiency, the *F*-value of 11.58 implied that the model was significant. The *p*-values less than 0.05 indicated that the model terms X_1, X_3, X_1^2, X_2^2 and X_3^2 were significant, as described in Table S2.

The suitability of the selected model for providing adequate estimations of real systems was also confirmed by normal probability plots of the studentised residuals and the predicted versus actual value plots, as shown in Figure S4(a) and S4(b), respectively (available online). It can be deduced

Table 2 | Design matrix in coded units and the experimental response

Run number	Current density (X_1)	Dosage (X_2)	Reaction time (X_3)	Removal efficiency (%, Y)
1	–1	1	1	69.5
2	1.682	0	0	82.5
3	–1	–1	1	67.0
4	0	0	1.682	89.3
5	–1.682	0	0	68.2
6	1	–1	–1	60.2
7	0	1.682	0	88.2
8	–1	1	–1	54.1
9	0	0	0	89.2
10	0	0	–1.682	47.3
11	0	0	0	88.9
12	0	–1.682	0	79.5
13	1	1	–1	63.4
14	0	0	0	90.5
15	0	0	0	90.7
16	0	0	0	91.2
17	1	1	1	88.2
18	–1	–1	–1	52.8
19	1	–1	1	70.4
20	0	0	0	90.2

from the plots that the data were evenly distributed. The model was tested using the determination coefficient (R^2). An R^2 value close to 1 indicates that the model is strong and gives good predictions of sulphate removal efficiency. The determination coefficient ($R^2 = 0.9253$) showed that only 7.47% of response variability was not explained by the model. In addition, the value of the adjusted determination coefficient ($R^2_{adj} = 0.8836$) was extremely high, thereby showing a high significance of the model. Moreover, the value of the predicted R^2 was high, thereby supporting the significance of the model. Thus, the predicted R^2 of 0.9075 for the model was in reasonable agreement with the adjusted R^2 of 0.8836. These results illustrate that the data prediction capability of the response surface model was satisfactory.

Interactive effects analysis and optimization

Contour plots of the mathematical regression model were described using Design Expert software to study the

interactive relationship between independent variables and response. Figure 5(a)–5(c) show the contour plots, where two variables were varied within the experimental range while the other variable was maintained constant. Figure 5(a) describes the interaction between the current density and dosage with a reaction time of 15 min. At dosage of 0.06 g/L, the removal efficiency increased by 22.54% (from 52.00 to 74.54%) and then decreased by 18.24% (from 74.54 to 56.3%) when the current density increased from 53.2 to 86.8 mA/cm^2; whereas at the dosage of 0.74 g/L, the removal efficiency increased by 35.65% (from 50.32 to 85.97%) and then decreased by 8.47% (from 85.97 to 77.5%) when the current density increased from 53.2 to 86.8 mA/cm^2.

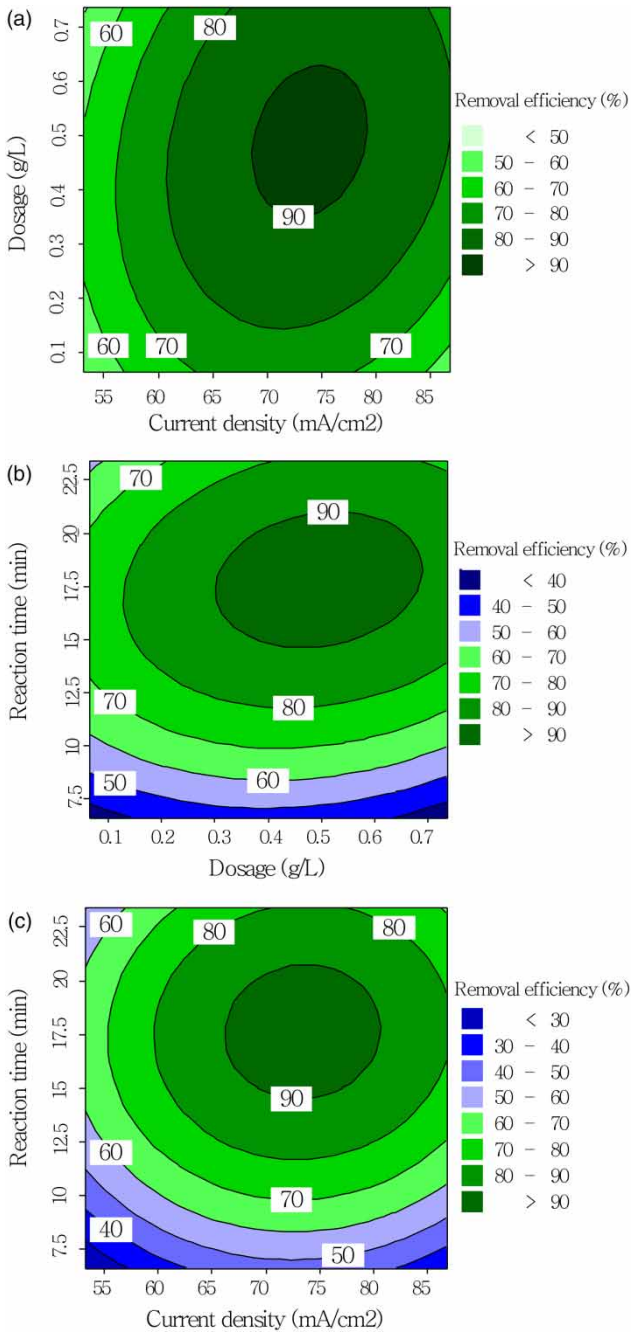

Figure 5 | Response surface plots for interactive effect among factors ((a)–(c): current density and RSAC dosage; reaction time and RSAC dosage; current density and reaction time) on sulphate removal efficiency.

The interaction between dosage and reaction time at the current density of 70 mA/cm^2 is illustrated in Figure 5(b). The plot shows that the removal efficiency increased by 11.72% (from 36.32 to 48.04%) and then decreased by 13.52% (from 48.04 to 34.52%) at a reaction time of 6.6 min; at a reaction time of 23.4 min, removal efficiency increased by 24.25% (from 57.99 to 82.24%) and then decreased by 3.57% (from 82.24 to 78.67%) when the dosage increased from 0.06 to 0.74 g/L.

Figure 5(c) illustrates the combined effects of current density and reaction time when the dosage was at zero level (0.4 g/L). At a reaction time of 6.6 min, the removal efficiency increased (from 21.56 to 47.23%) when the current density increased from 53.2 to 70 mA/cm^2 and then decreased (from 47.23 to 32.48%) until 86.8 mA/cm^2; at a reaction time of 23.4 min, the removal efficiency increased (from 50.1 to 81.25%) when the current density increased from 53.2 to 70 mA/cm^2 and then decreased (from 81.25 to 69.84%) until 86.8 mA/cm^2.

In summary, sulphate removal was targeted as maximum based on the response surface and desirability functions to optimise the model. The optimal results for sulphate removal efficiency were predicted to occur under the following conditions: a current density of 75 mA/cm^2, a dosage of 0.46 g/L and a reaction time of 19.2 min. The actual value of sulphate removal efficiency was 95.2% with a relatively small error, which was in good agreement with the predicted value (94.08%) from the regression model.

Economic and technical analysis

The calculated cost of current, voltage and reaction time was considered in the assessment of the described EC/RSAC coupled system. In this study, current density and reaction time at the optimum operating conditions were 75 mA/cm^2 and 19.2 min, respectively. For this current density, current

Table 3 | Comparison of EC/RSAC and other different EC systems for sulphate removal

Initial sulphate concentration (mg/L)	Removal efficiency (%)	Operational parameters	References
2,650	40	Current density 180 A/m^2, time 180 min, Fe-Fe electrodes	Jo *et al.* (2016)
54	59	Current density 47 mA/cm^2, time 20 min, Fe-Al electrodes	Murugananthan *et al.* (2004)
13,000	28.9, 40.5	Current density 70 mA/cm^2, time 120 min, Fe-Fe, Al-Al electrodes	Nariyan *et al.* (2017)
13,000 (1,600 mg/L after chemical precipitation)	84.4	Current density 25 mA/cm^2, time 240 min, Fe-Al electrodes	Nariyan *et al.* (2018)
2,973.22	95.2	Current density 75 mA/cm^2, time 19.2 min, Fe-Al electrodes, RSAC dosage 0.46 g/L	Current work

and voltage values were 3 A and 11.2 V, respectively. Based on these values, the energy consumption (ECC) can be estimated by the following equation:

$$ECC = (UIt)/v \tag{11}$$

where U, I, t and v are the voltage (V), current (A), reaction time (h) and effluent volume (m^3), for the EC process. Based on the China market in 2017, the electricity cost was \$0.049/kwh. The cost of EC was estimated as \$2.42/m^3 for mine waters treatment.

The performances of the EC/RSAC coupling system under optimized conditions and the former EC systems are shown in Table 3. Compared with the former EC technologies, RSAC/EC exhibited the highest sulphate removal rate and the lowest reaction time.

CONCLUSION

In this work, the EC/RSAC adsorption coupled process was applied for the removal of sulphate from mine water in a batch experiment. The addition of RSAC as adsorbent resulted in a higher removal efficiency (51.7%), especially at a short reaction time (10 min), compared with the conventional EC process (24.3%). The success of this coupled system is linked to the specific characteristic of the adsorbent. A response surface method based on a three-variable (i.e. current density, RSAC dosage and reaction time), five-level central composite experiment design was successfully employed in this optimisation study. Regression analysis revealed the good fit of the experimental data to a second-order polynomial model with a coefficient of determination (R^2) value of 0.9253 and an F value of 11.58. The ANOVA results showed that current density (X_1) and reaction time (X_3) possessed high F values (7.88 and 36.46), which implies that they were significant factors affecting sulphate removal efficiency. The maximum removal efficiency of 95.2% was obtained under the following optimal parameters: current density of 75 mA/cm^2, RSAC dosage of 0.46 g/L and reaction time of 19.2 min. The RSM prediction value (94.08) is consistent with the measured experimental results to a considerable degree with a slight deviation. The findings of this study show that sulphate can be efficiently removed from aqueous solutions using EC/RSAC technology. The findings also provide the theoretical basis for solving the problem of mine wastewater industries.

ACKNOWLEDGEMENTS

We gratefully acknowledge the financial support provided by the National Science and Technology Major Project of China (2016ZX05025-003) and the National Natural Science Foundation of China (41773133, 41273131). We also thank Dr Geoffrey I. Sunahara for valuable suggestions for the paper.

REFERENCES

Akbal, F. & Camc, S. 2011 Copper, chromium and nickel removal from metal plating waste water by electrocoagulation. *Desalination* **269** (1–3), 214–222.

Avsar, Y., Kurt, U. & Gonullu, T. 2007 Comparison of classical chemical and electrochemical processes for treating rose processing wastewater. *J. Hazard. Mater.* **148** (1–2), 340–345.

Bayar, S., Yıldız, Y. Ş., Yılmaz, A. E. & Şahset, İ. 2011 The effect of stirring speed and current density on removal efficiency of poultry slaughterhouse wastewater by electrocoagulation method. *Desalination* **280** (1), 103–107.

Bayramoglu, M., Kobya, M., Can, O. T. & Sozbir, M. 2004 Operating cost analysis of electrocoagulation of textile dye wastewater. *Sep. Purif. Technol.* **37** (2), 117–125.

Canizares, P., Martinez, F., Lobato, J. & Rodrigo, M. 2006 Electrochemically assisted coagulation of wastes polluted with eriochrome Black T. *Ind. Eng. Chem. Res.* **45** (10), 3474–3480.

Carvalho, H. P. D., Huang, J. G., Zhao, M. X., Liu, G., Dong, L. L. & Liu, X. J. 2015 Improvement of Methylene Blue removal by electrocoagulation/banana peel adsorption coupling in a batch system. *Alex. Eng. J.* **54** (3), 777–786.

Chen, X., Chen, G. & Yue, P. L. 2007 Separation of pollutants from restaurant wastewater by electrocoagulation. *Sep. Sci. Technol.* **42** (4), 819–833.

Elnenay, A. M. H., Nassef, E., Malash, G. F. & Magid, M. H. A. 2017 Treatment of drilling fluids wastewater by electrocoagulation. *Egypt. J. Petro.* **26** (1), 203–208.

Farahmand, E., Rezai, B., Doulati, A. F. & Shafaei, T. S. Z. 2015 Kinetics, equilibrium, and thermodynamic studies of sulphate adsorption from aqueous solution using activated carbon derived from Rice Straw. *Bulg. Chem. Commun.* **47**, 72–81.

Franco, D., Lee, J., Arbelaez, S., Cohen, N. & Kim, J. Y. 2017 Removal of phosphate from surface and wastewater via electrocoagulation. *Ecol. Eng.* **108** (B), 589–596.

Gärtner, R. S., Wilhelm, F. G., Witkamp, G. J. & Wessling, M. 2005 Regeneration of mixed solvent by electrodialysis: selective removal of chloride and sulfate. *J. Membr. Sci.* **250** (1), 113–133.

Greben, H. A., Baloyi, J., Sigama, J. & Venter, S. N. 2009 Bioremediation of sulphate rich mine effluents using grass cuttings and rumen fluid microorganisms. *J. Geochem. Explor.* **100** (2), 163–168.

Guimarães, D. & Leão, V. A. 2014 Batch and fixed-bed assessment of sulphate removal by the weak base ion exchange resin Amberlyst A21. *J. Hazard. Mater.* **280**, 209–215.

Guvenc, S. Y., Okut, Y., Ozak, M., Haktanir, B. & Bilgili, M. S. 2017 Process optimization via response surface methodology in the treatment of metal working industry wastewater with electrocoagulation. *Water Sci. Technol.* **75** (4), 833–846.

Hallajiqomi, M. & Eisazadeh, H. 2017 Adsorption of manganese ion using polyaniline and its nanocomposite: kinetics and isotherm studies. *J. Ind. Eng. Chem.* **55**, 191–197.

Iii, C. A. C. & Trahan, M. K. 1999 Limestone drains to increase pH and remove dissolved metals from acidic mine drainage. *Appl. Geochem.* **14** (5), 581–606.

Jo, E. Y., Park, S. M., Yeo, I. S., Cha, J. D., Lee, J. Y., Kim, Y. H., Lee, T. K. & Park, C. G. 2016 A study on the removal of sulfate and nitrate from the wet scrubber wastewater using electrocoagulation. *Desal. Water Treat.* **57** (17), 7833–7840.

Kefeni, K. K., Msagati, T. A. M. & Mamba, B. B. 2017 Acid mine drainage: prevention, treatment options, and resource recovery: a review. *J. Clean. Prod.* **151** (10), 475–493.

Kobya, M., Senturk, E. & Bayramoglu, M. 2006 Treatment of poultry slaughterhouse wastewaters by electrocoagulation. *J. Hazard. Mater.* **133** (1–3), 172–176.

Kumar, P. R., Chaudhari, S., Khilar, K. C. & Mahajan, S. P. 2004 Removal of arsenic from water by electrocoagulation. *Chemosphere* **55** (9), 1245–1252.

Mamelkina, M. A., Cotillas, S., Lacasa, E., Sáez, C., Tuunila, R., Sillanpää, M., Häkkinen, A. & Rodrigo, M. A. 2017 Removal of sulfate from mining waters by electrocoagulation. *Sep. Purif. Technol.* **182**, 87–93.

Martins, M., Faleiro, M. L., Barros, R. J., Veríssimo, A. R., Barreiros, M. A. & Costa, M. C. 2009 Characterization and activity studies of highly heavy metal resistant sulphate-reducing bacteria to be used in acid mine drainage decontamination. *J. Hazard. Mater.* **166** (2–3), 706–713.

Murugananthan, M., Raju, G. B. & Prabhakar, S. 2004 Removal of sulfide, sulfate and sulfite ions by electro coagulation. *J. Hazard. Mater.* **109** (1), 37–44.

Najib, T., Solgi, M., Farazmand, A., Heydarian, S. M. & Nasernejad, B. 2017 Optimization of sulfate removal by sulfate reducing bacteria using response surface methodology and heavy metal removal in a sulfidogenic UASB reactor. *J. Environ. Chem. Eng.* **5** (4), 3256–3265.

Namasivayam, C. & Sangeetha, D. 2008 Application of coconut coir pith for the removal of sulfate and other anions from water. *Desalination* **219** (1), 1–13.

Nariyan, E., Sillanpää, M. & Wolkersdorfer, C. 2017 Electrocoagulation treatment of mine water from the deepest working European metal mine-performance, isotherm and kinetic studies. *Separ. Purif. Technol.* **177**, 363–373.

Nariyan, E., Wolkersdorfer, C. & Sillanpää, M. 2018 Sulfate removal from acid mine water from the deepest active European mine by precipitation and various electrocoagulation configurations. *J. Environ. Manag.* **227**, 162–171.

Papirio, S., Villa-Gomez, D. K., Esposito, G., Pirozzi, F. & Lens, P. N. L. 2013 Acid mine drainage treatment in fluidized-bed bioreactors by sulfate-reducing bacteria: a critical review. *Crit. Rev. Environ. Sci. Technol.* **43** (23), 2545–2580.

Paz-García, J. M., Johannesson, B., Ottosen, L. M., Ribeiro, A. B. & Rodríguez-Maroto, J. M. 2013 Simulation-based analysis of the differences in the removal rate of chlorides, nitrates and sulfates by electrokinetic desalination treatments. *Electrochim. Acta* **89** (3), 436–444.

Runtti, H., Tynjälä, P., Tuomikoski, S., Kangas, T., Hu, T., Rämö, J. & Lassi, U. 2017 Utilisation of barium-modified analcime in sulphate removal: isotherms, kinetics and thermodynamics studies. *J. Water Process Eng.* **16**, 319–328.

Sahu, O., Mazumdar, B. & Chaudhari, P. K. 2014 Treatment of wastewater by electrocoagulation: a review. *Environ. Sci. Pollut. Res.* **21** (4), 2397–2413.

Silva, R., Cadorin, L. & Rubio, J. 2010 Sulphate ions removal from an aqueous solution: I. Co-precipitation with

hydrolysed aluminum-bearing salts. *Miner. Eng.* **23** (15), 1220–1226.

Silva, A. M., Lima, R. M. & Leão, V. A. 2012 Mine water treatment with limestone for sulfate removal. *J. Hazard. Mater.* **221–222** (30), 45–55.

Sundaramurthy, S., Rajesh, P. & Prasad, B. 2012 Use of granular activated carbon for the enhancement of phenol. *Int. J. Biol. Sci. Eng.* **3**, 223–228.

Vivek, N. N. & Ganesan, M. 2009 Use of adsorption using granular activated carbon (GAC) for the enhancement of removal of chromium from synthetic wastewater by electrocoagulation. *J. Hazard. Mater.* **161** (1), 575–580.

Zaied, M. & Bellakhal, N. 2009 Electrocoagulation treatment of black liquor from paper industry. *J. Hazard. Mater.* **163** (2–3), 995–1000.

Zhu, M. J., Liu, R. P., Chai, H. K., Yao, J., Chen, Y. P. & Yi, Z. J. 2016a Hazelnut shell activated carbon: a potential adsorbent material for the decontamination of uranium(VI) from aqueous solutions. *J. Radioanal. Nucl. Chem.* **310** (3), 1147–1154.

Zhu, M. J., Yao, J., Wang, W. B., Yin, X. Q., Chen, W. & Wu, X. Y. 2016b Using response surface methodology to evaluate electrocoagulation in the pretreatment of produced water from polymer-flooding well of Dagang Oilfield with bipolar aluminum electrodes. *Desal. Water Treat.* **57** (33), 15314–15325.

First received 14 August 2018; accepted in revised form 5 November 2018. Available online 11 December 2018